Efficient Method for Prediction of Stability in Low Immersion Milling

B. Moetakef Imani
Mech. Eng. Group
Ferdowsi Univ. of Mashhad

M.H. Sadeghi
Mech. Eng. Group
Tarbiat Modarres Univ.

M. Kazemi Nasrabadi
Mech. Eng. Group
Shahid Sattari Air Univ.

ABSTRACT
This paper presents cutting force prediction algorithm for low immersion end-milling, using an efficient dynamic force modeler. The geometric simulation of milling process was performed, using the B-Rep solid modeling techniques. For predicting stability lobes, two methods were used for prediction of stability lobes: the frequency domain technique and the time finite element analysis (TFEA). The frequency domain technique is faster and except for low immersion milling, is accurate. The TFEA method forms an approximate solution by dividing the cutting time into a finite number of elements. This approximated solution is then matched with the exact one for free vibration to obtain a discrete linear map. The comprehensive time domain simulation is used, in order to verify stability lobes diagram obtained by frequency domain technique and TFEA method.

Key Words: Stability Limit, Low Immersion Milling, ACIS

روش مؤثر برای پیش‌بینی پایداری در فرزکاری با بار جانبی کم

بهنام معتکف ایمانی[1]
گروه مهندسی مکانیک
دانشگاه فردوسی مشهد

محمد حسین صادقی[2]
گروه مهندسی مکانیک
دانشگاه تربیت مدرس

محمد کاظمی نصرآبادی[3]
گروه مهندسی مکانیک
دانشگاه هوایی شهید ستاری

(تاریخ دریافت: ۱۳۸۵/۱۲/۰۱؛ تاریخ پذیرش: ۱۳۸۶/۰۶/۰۳)

چکیده
در این مقاله، با استفاده از مدل نیروی دینامیکی کارآمد، نیروهای فرزکاری با بار جانبی کم ارائه می‌شوند. شبیه‌سازی هندسی فرآیند فرزکاری با استفاده از تکنیک‌های مدل‌سازی صلب B-Rep صورت می‌گیرد. روش‌های دامنه فرکانسی و آنالیز المان محدود زمانی (TFEA) برای پیش‌بینی دالان‌های پایداری استفاده شده است. روش دامنه فرکانسی سریع‌ترین روشی است که به جز برای موارد فرزکاری با بار جانبی کم، دقیق نیز می‌باشد. روش TFEA یک حل تقریبی با تقسیم نمودن زمان درگیری و برش به تعداد محدودی المان زمانی ارائه می‌نماید. حل تقریبی با حل کامل برای ارتعاشات آزاد مطابقت داده می‌شود تا دیاگرام خطی مجزا به دست آید. شبیه‌سازی جامع حوزه زمان به منظور تأیید دالان‌های پایداری به دست آمده از روش‌های حوزه فرکانسی و TFEA به کار می‌رود.

واژه‌های کلیدی: محدوده پایداری، فرزکاری با بار جانبی کم، ACIS

1- Associate Professor
2- Associate Professor
3- Assistant Professor (Corresponding Author): m_nasr1350@yahoo.com

1. Introduction

Maximizing productivity is the main goal in the machining processes. For the milling process, this is equivalent to maximizing the material removal rate (MRR). There are several methods for increasing the MRR: 1) increasing the feed rate, 2) increasing the cutting depth, and 3) increasing the spindle speed.

Recent advances in machine technology have enabled the machine tool manufacturers to produce machines with spindle speeds exceeding 40,000 rpm [1]. High speed machining (HSM) enables very high MRR for milling operations. Although the definition of HSM is not so clear, it is usually related to spindle speed. A useful definition proposed by smith [2] is "machining at or near the resonant frequencies of the tool or machine"

HSM is vastly used in aerospace industries in order to produce flexible parts such as different kinds of blades, fuselage components, and thin wall housings, there are several advantages for HSM. In comparison with conventional milling. the main one is improving the production speed or MRR. In addition, cutting forces and required, the power will be reduced to some extent. Also, it is possible to manufacture thin wall housings out of a single block instead of assembling the from several parts. These parts are simultaneously lighter, stronger, cheaper and require a small fraction of the machining time compared to the conventional machining techniques [1].

There has been quite significant research for predicting of machining forces with various levels of accuracy and complexity [3, 4]. These force models can be categorized as follows: 1) rigid force model, 2) flexible force model and 3) regenerative force model.

In the present study, the geometric simulation of milling process is performed using B-Rep solid modelling techniques [5]. The geometric modeller must be capable of representing valid model of part and tool, updating the model of part throughout the machining operations, and constructing entities required in machining simulations such as cutting edges and chip geometries. The current work incorporates ACIS[1] for the task of geometric simulations [5].

HSM demands an accurate mathematical model of milling process in order to predict stability limits of the self excited type of vibrations which is called chatter. Stability limits (or lobes) separate stable and unstable machining regions and provide practical guide for optimum machine and tool planning. There are two types of stability lobes: those related to secondary Hopf bifurcation, and those related to period doubling (or flip) bifurcations. For the case of flip lobes, the chatter frequencies linearly depend on the spindle speed and for the Hopf lobes, the number of chatter frequencies are duplicated. Two methods are suggested for predicting the stability lobes: 1) frequency domain with a continuous cutting model or an interrupted cutting model [6] and 2) time domain simulation, [7, 8]. Prediction of stability lobes using frequency domain requires the transfer function matrix at the cutter-workpiece contact location and also the dynamic cutting coefficient for the given cutting condition, [9]. A newly proposed method incorporates time finite element analysis (TFEA) to solve the delayed differential equation of motion which can accurately solve the low immersion milling dynamics, [10,11]. In this method, cutting time is divided into a number of elements, where displacement and velocity continuity are enforced between each element. An approximate discrete linear map is then constructed using time finite elements in the cut to exact mapping of free vibration out of the cut. In this way, stability lobes can be predicted from the eignvalues of the discrete map. Henceforth, the paper is organized as follows: the required geometric simulations are presented in section 2. The importance and efficiency of geometric simulation in force modeling are clarified in section 3. Mathematical model of 2DOF milling dynamics is investigated in section 4 which was simulated using MATLAB software [12]. The mechanics of low immersion milling operation is discussed in section 5. Dynamic modeling of milling operations is done in section 6. In the following section stability lobe diagrams are obtained using frequency domain method and TFEA. Sections 8 and 9 show the results of different methods and compare them with the time domain simulation results. Lastly, section 10 concludes the results obtained in this research.

2. Geometric Simulation

During milling process, the portion of the tool cutting edge that is engaged to workpiece at a given instant of time, is defined as tool engagement. Milling free-form surfaces, the tool engagement varies along the tool path. The variation of tool engagement results in corresponding variation in the cutting forces. In some cases, sudden increase in tool engagement may even result in tool breakage. Therefore, tool engagement must be accurately identified in order to predict cutting forces. Tool engagement is influenced by the radial and axial cutting depth of cut which are defined in Fig. **1**.

1- B-rep Solid Modeler

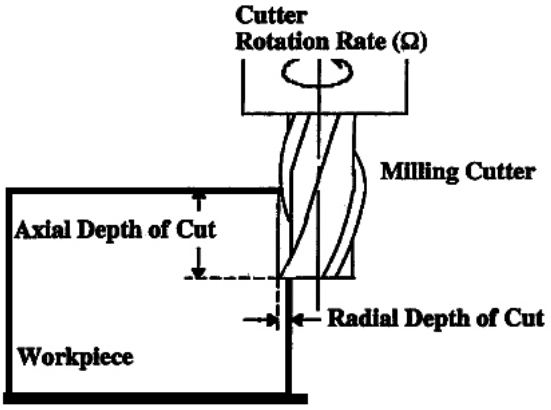

Fig. (1): Tool engagement in milling operation**.**

In order to calculate the tool engagement geometry at a given instant, is required geometric simulation of milling operations. For performing this, ACIS, a B-Rep solid modeler, is used. The end milling tool is represented by a cylinder with the diameter and height equal to the diameter and cutting length of the end mill. The cutting edge is modeled by a NURBS[2] curve. The tool and cutting edge are illustrated in Fig. **2**.

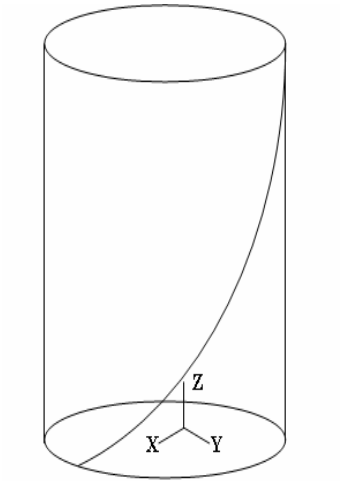

Fig. (2): Cutting edge of end mill.

The part is updated as the tool cuts the part material. In order to update the part, the swept volume of the tool along the tool path is required. Fig. **3** shows the swept volume of a linear tool path which has been divided to three sections. 1- semi-cylinder at the start point 2- swept volume of tool envelope 3- semi-cylinder at the end point. These three volumes are united and subtracted from the model due to updating the part.

2 - Non-uniform Rational B-spline

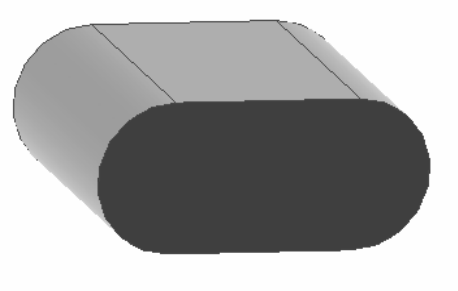

Fig. (3): Swept volume of tool.

The contact face and its boundary edges: AB, BC, CD, and DA are depicted in Fig. **4**. The intersection points of the helical edge with the contact face boundaries are also shown in the same figure.

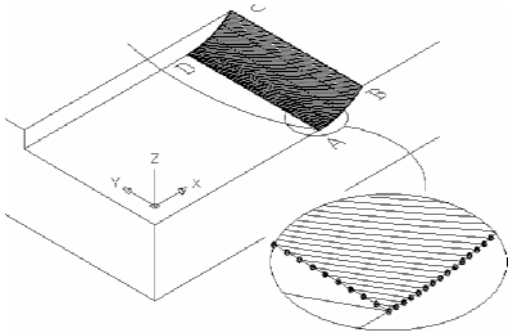

Fig. (4): Edge engagement with workpiece**.**

The boundaries AB and BC of the contact face identify the start coordinates of edge engagement, and the boundaries CD and DA show the end coordinates of edge engagement. For down milling, these tool engagement starts from the point C and finishes at the point A, while for up milling, these points play reverse roes. The entry and exit angles of cutting edge at each instant can be calculated as follows:

$$\sin\phi = \frac{x}{r} \;\Rightarrow\; \sin\phi_s = \frac{x_s}{r} \Rightarrow \sin^{-1}\frac{x_s}{r} \qquad \sin\phi_e = \frac{x_e}{r} \Rightarrow \sin^{-1}\frac{x_e}{r}. \tag{1}$$

3. Importance of Geometric Simulation in Force Modeling

The simulation process in ACIS software, leads to the simulation of milling operation for complicated parts, see [13] for detail:

1- During the milling operation on complicated surfaces, there is no analytical relationship for calculating the entry and exit angle or for predicting the chip loads and only they can only be predicted by means of solid modeling software,

2- There is a high ability in ACIS software for predicting or calculating the instantaneous chip loads for complicated cutting edges geometry as same as the ball nose, tapered ball nose or roughing

end mills and
3- When workpiece or tool are flexible, the tool-workpiece contact face will vary during the cutting operation due to the dynamic deflections. ACIS will simplify the modeling of contact face and consequently will calculate the entry and exit angles accurately.

4. Mathematical Model of 2- DOF End Milling

A schematic diagram of a two-degree-of-freedom milling process is shown in Fig. **5**.

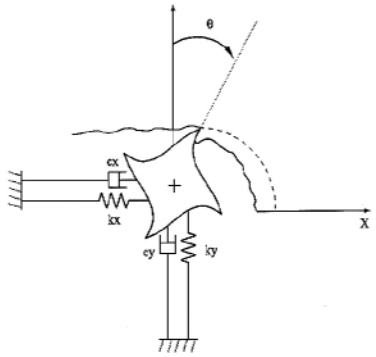

Fig. (5): 2-DOF model of end milling.

Tool and structure are modeled by a single mode vibration in two uncoupled and orthogonal directions. The differential equation of motion is given by [12]:

$$M\ddot{X}(t) + C\dot{X}(t) + KX(t) = F(t), \quad (2)$$

where, $X(t) = [x(t) \;\; y(t)]^T$ is the two-element position vector and M, C, and K are mass, damping, and stiffness matrices, respectively.
The x and y cutting force components on the pth tooth are given by [12]:

$$\begin{aligned} F_{xp}(t) &= [-F_{tp}(t)\cos\theta_p(t) - F_{np}(t)\sin\theta_p(t)]g_p(t), \\ F_{yp}(t) &= [F_{tp}(t)\sin\theta_p(t) - F_{np}(t)\cos\theta_p(t)]g_p(t), \end{aligned} \quad (3)$$

where, $g_p(t)$ acts as a switching function equal to one if the pth tooth is in-cut and zero if it is not cutting. The tangential and normal cutting force components, F_{tp} and F_{np} respectively, are considered to be the product of linearized cutting coefficients K_t and K_n, the nominal depth of cut (DOC) and the instantaneous chip width $w_p(t)$:

$$\begin{aligned} F_{t,p}(t) &= K_t.doc.w_p(t), \\ F_{r,p}(t) &= K_n.doc.w_p(t), \end{aligned} \quad (4)$$

where, $w_p(t)$ depends upon the feed per tooth, f_t, the cutter rotation angle $\theta_p(t)$ and regeneration in the compliant structure directions:

$$\begin{aligned} w_p(t) = f_t \sin\theta_p(t) &+ [x(t) - x(t-\tau)]\sin\theta_p(t) \\ &+ [y(t) - y(t-\tau)]\cos\theta_p(t). \end{aligned} \quad (5)$$

In the above relationship, $f_t \sin\theta_p(t)$ represents the circular tool path approximation of chip thickness and τ is tooth passing period and given by $\tau = 2\pi / Nn \; [s]$, where n is the spindle speed given in rpm and N is the total number of cutting teeth. The angular position of the pth tooth for a tool with evenly spaced teeth is:

$$\theta_p(t) = \Omega t + 2\pi(p-1)/N, \; p = 1,2,3,...,N, \quad (6)$$

as $\Omega = \dfrac{2\pi n}{60}$. The total cutting force equations are found by summing the forces on each cutting tooth and substituting equations (4) and (5) into (3):

$$\begin{aligned} \begin{bmatrix} F_x \\ F_y \end{bmatrix} &= \sum_{p=1}^{N} g_p(t).doc.(f_t \begin{bmatrix} -K_t sc & -K_n s^2 \\ K_t s^2 & -K_n sc \end{bmatrix} \\ &+ \begin{bmatrix} -K_t sc - K_n s^2 & -K_t c^2 - K_n sc \\ K_t s^2 - K_n sc & K_t sc - K_n c^2 \end{bmatrix} \begin{bmatrix} \Delta x \\ \Delta y \end{bmatrix}, \end{aligned} \quad (7)$$

where, $s = \sin\theta_p(t)$, $c = \cos\theta_p(t)$
and $\Delta x = x(t) - x(t-\tau)$, $\Delta y = y(t) - y(t-\tau)$.
Finally, the comprehensive equation of motion can be expressed by Eq. (10), where $f_\circ(t)$ and $K_c(t)$ are given by:

$$f_\circ(t) = \sum_{p=1}^{N} g_p(t) f_t \begin{bmatrix} -K_t sc & -K_n s^2 \\ K_t s^2 & -K_n sc \end{bmatrix}, \quad (8)$$

$$K_c(t) = \sum_{p=1}^{N} g_p(t) \begin{bmatrix} -K_t sc - K_n s^2 & -K_t c^2 - K_n sc \\ K_t s^2 - K_n sc & K_t sc - K_n c^2 \end{bmatrix}, \quad (9)$$

$$\begin{aligned} &M\ddot{X}(t) + C\dot{X}(t) + KX(t) = \\ &K_c(t).doc.[X(t) - X(t-\tau)] + f_\circ(t).doc. \end{aligned} \quad (10)$$

$K_c(t)$ and $f_\circ(t)$ are periodic functions with the same period of tool passing. Since the cutting stability has been influenced only by the dynamic part of chip thickness, in Eq. (10) $f_\circ(t).doc$ term can be ignored and the final equation of motion is presented by [14]:

$$\begin{aligned} &M\ddot{X}(t) + C\dot{X}(t) + KX(t) = \\ &K_c(t).doc.[X(t) - X(t-\tau)]. \end{aligned} \quad (11)$$

When the structure is only compliant in a single direction, equation (10) can be modified by eliminating the corresponding rows and columns of the rigid direction. For instance, a structure compliant only in the x direction would have the following equation of motion:

$$\ddot{X}(t)+2\xi\omega_n\dot{X}(t)+\omega_n^2X(t)= \frac{K_{sx}(t).doc}{m}[X(t)-X(t-\tau)]. \quad (12)$$

Fig. **6**. presents the specific cutting force variation $K_s(t)$ for different partial immersion up-milling operation for a two fluted tool. The following experimentally identified parameters were used:

$K_t = 5.5\times10^8 N/m^2$, $K_n = 2\times10^6 N/m^2$.

The discontinuity of the function is due to the tooth passing effect. In the half immersion case, the entry and exit angles are 0° and 90°, respectively. If the angular position of the teeth are $90^\circ < \varphi_1 < 180^\circ$ and $270^\circ < \varphi_2 < 360^\circ$, then both teeth are out of cut and the function $K_s(t)$ would be zero [15].

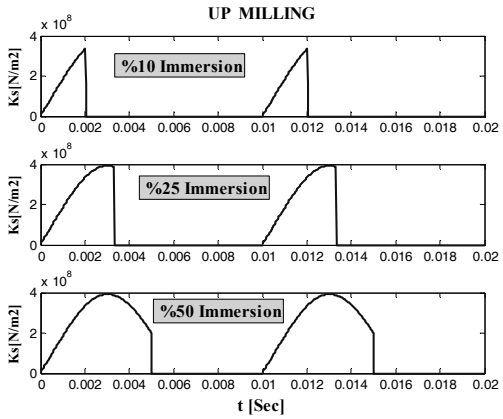

Fig. (6): Specific cutting force variation.

5. Low Immersion

The radial depth of cut plays an important role in milling forces, because as the radial depth of cut is increased, the contact area increases and cutting force magnitude becomes larger. Recent findings indicate that tool wear rate for difficult-to-cut materials such as titanium alloys, decreases significantly along with the radial immersion decrease [16]. Thus, the time domain simulations are performed for six immersion cases. Tool geometrics and cutting conditions are given in table **1**. The simulations are performed based on the methodology proposed in section 4. The results of the action are illustrated in Fig. **7**. In each figure the resultant of cutting forces, in x and y directions is also presented. In this figure, it is demonstrated that since the contact area is increased by accruing the radial depth of cut. The milling forces increase as well. More over, when the axial depth of cut is increased, the length of engaged flutes increases, and the milling forces increase. But the effect of radial depth of cut on increasing the cutting forces is more pronounced than that of the axial depth of cut. Again, it shows that the shape of the measured force becomes smooth when axial depth of cut increases. This is due to the cutting edge engagement, when the axial depth of cut is large and the engaged length of the edge is constant.

Table (1): Parameters used in milling Process.

Axial depth of cut	DOC=5 , 6 , 7 , 8 mm
Radial depth of cut	WOC=1 , 2, 3 mm
Average specific cutting coefficient (Ti-6Al-4V)	Ks=1356 (N/mm^2)[10]
Number of tooth	N=4
Helix angle	$\beta = 30^\circ$
Feed per tooth	$f_t = 0.05\,mm$
Tool diameter	D=8 mm

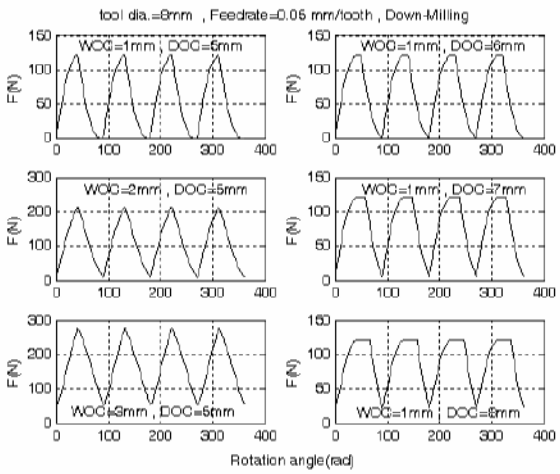

Fig. (7): Simulated forces with different immersions.

6. Dynamic Modeling of Milling Operations

In this section, chip load is computed by ACIS and the algorithms given by [17-20]. ACIS is a B-Rep solid modeler and can vigorously compute chip load for any shape of tool path and work piece geometriy, Further detail can be found in [13, 21]. F_X, F_Y and F force components for different immersions are presented by useing two methods. In order to study the frequency components of the cutting force, the FFT of the resultant force has been presented. The assuming parameter given in table **2**, figures 8-10 illustrates the results of simulation for the given cutting conditions. It is obvious that in a stable machining operation, the dominant frequency is the tool passing frequency, which can be calculated by:

$$Tool\ Pass\ \ Frequency\ \ [HZ] = \frac{nN}{60}\ . \quad (13)$$

Table (2): Cutting conditions and modal parameters.

Tool diameter	D=8mm
Number of tooth	N=4
Feed per tooth	F_t=0.1 mm
Cutting Coefficient	$K_t = 2\times10^9 N/m^2$ $K_n = 6.6\times10^8 N/m^2$
Modal Parameters	f_x , $f_y = 660 Hz$ k_x , $k_y = 2\times10^7 N/m$ ξ_x , $\xi_y = 0.05$

As illustrated in figures, by increasing WOC to 3mm, the amplitude of cutting force increases significantly and the system becomes unstable. FFT of the cutting shows that the this instability is due the chatter frequency close to the most flexible mode shape.

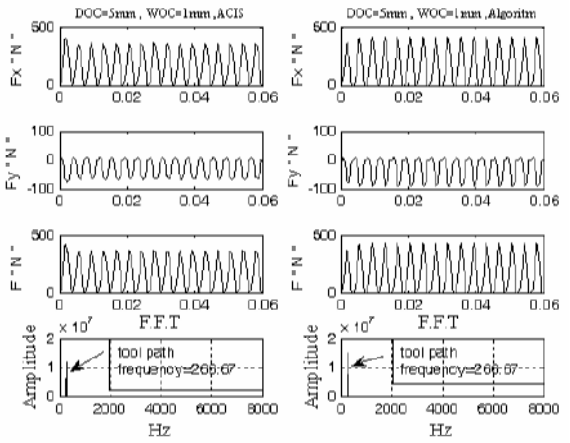

Fig. (8): Up-milling, axial depth of cut =5 mm, radial depth of cut = 1mm.

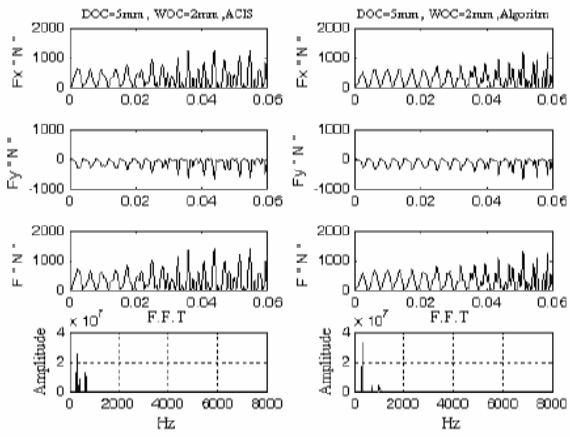

Fig. (9): up-milling, axial depth of cut =5 mm, radial depth of cut = 2mm.

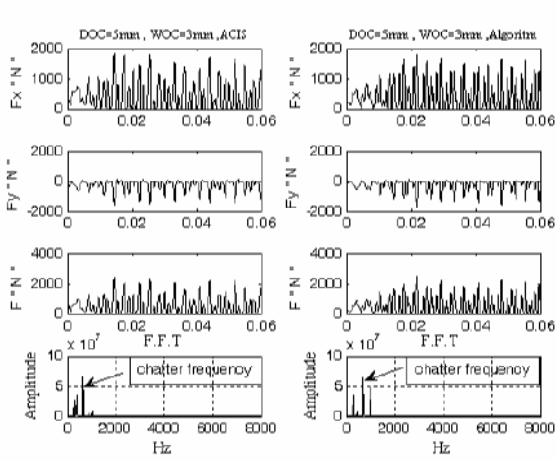

Fig. (10): up-milling, axial depth of cut =5 mm, radial depth of cut = 3mm.

7. Stability Lobes

There are two main differences in the stability of low immersion milling:

1- The equation of motion when edge is not engaged is free vibration and

2- There is no exact analytical solution when the tool is in the cut.

The stability limit diagram (SLD) differentiates two region: stable cutting and instability due to chatter vibrations where variations of DOC versus spindle speed is taken into consideration at onset of chatter vibrations. By means of SLD, optimum parameters which provide maximum material removal rate without chatter, can be seen.

There are two kinds of instability in low immersion milling. In this part, SLD are obtained using two methods. Frequency domain [22] and TFEA [23-24]. The main reason here is to find an efficient method for obtaining SLD of low immersion milling operations.

7.1 Calculation of Stability Lobes by Frequency Domain Method

The frequency domain method can compute SLD of machining operation system using frequency response function (FRF) determined at the end of the tool. In order to compute FRF, an accelerometer is mounted at the end of the tool in x one, and it is excited by means of a hammer in the same direction. The same procedure is also performed for the y direction. In addition to direction FRF ($i.e.\ \phi_{xx}\ and\ \phi_{yy}$), cross FRF ($\phi_{xy}\ and\ \phi_{yx}$) can be obtained using same procedure.

The transfer function matrix which related forces to displacements at tool tip is expressed by [25]:

$$[\phi(i\omega)] = \begin{bmatrix} \phi_{xx}(i\omega) & \phi_{xy}(i\omega) \\ \phi_{yx}(i\omega) & \phi_{yy}(i\omega) \end{bmatrix} . \qquad (14)$$

7.2. TFEA method

The dynamic behavior of the milling process is governed by Eq. (10). Since this equation does not have a closed form solution, an approximate solution is sought to understand the behavior of the system. One such technique used for dynamic system is time finite element analysis (TFEA) [26]. This method was first applied for an interrupted turning process by Bayly et al [27]. In low-radial immersion milling, or for any cut less than a full immersion, the tool switches between cutting and not cutting. When the tool is out of the cut, the free vibrations can be described exactly with a closed form solution. But during cutting, there is no exact solution due to the existence of time-delayed terms. TFEA can break time in the cut into multiple elements and approximate the vector displacement on a single element as a linear combination of polynomial trial functions [28].

7.2.1 Free Vibration

When the tool is not in contact with the workpiece, the system experiences free vibration:

$$m\ddot{x}(t) + c\dot{x}(t) + kx(t) = 0 \quad . \tag{15}$$

which has the exact solution as follows: $x(t) = c_1 e^{\lambda_1 t} + c_2 e^{\lambda_2 t}$.

where, $\lambda_{1,2} = -\xi\omega_n \pm i\omega_d$ and $\omega_d = \omega_n\sqrt{1-\xi^2}$ is damped natural angular frequency. If we let t_c duration of cutting and t_f duration of free vibration, a state transition matrix can be obtained relating the final state of free vibration to the initial state [10]:

$$\begin{Bmatrix} x(t_c + t_f) \\ v(t_c + t_f) \end{Bmatrix} = \frac{1}{\lambda_2 - \lambda_1} \begin{bmatrix} -\lambda_1 e^{\lambda_2 t_f} + \lambda_2 e^{\lambda_1 t_f} & -e^{\lambda_1 t_f} + e^{\lambda_2 t_f} \\ -\lambda_1\lambda_2 e^{\lambda_2 t_f} + \lambda_1\lambda_2 e^{\lambda_1 t_f} & -\lambda_1 e^{\lambda_1 t_f} + \lambda_2 e^{\lambda_2 t_f} \end{bmatrix} \begin{bmatrix} x(t_c) \\ v(t_c) \end{bmatrix}. \tag{16}$$

7.2.2 Vibration During Cutting

When the tool is in-cut, an approximate solution for displacement of the tool during the j_{th} element of the n_{th} period of revolution can be assumed by: $\mathbf{X}(t) = \sum_{i=1}^{4} \mathbf{a}_{ji}^{n} \phi_i(\sigma_j(t))$. Here $\sigma_j(t) = t - n\tau - \sum_{k=1}^{j-1} t_K$ is the "local" time within the j_{th} element of the n_{th} period, the length of the k_{th} element is t_k and the trial functions $\phi_i(\sigma_j(t))$ are the cubic Hermit polynomials [29]:

$$\begin{aligned} \phi_1(\sigma_j) &= 1 - 3(\frac{\sigma_j}{t_j})^2 + 2(\frac{\sigma_j}{t_j})^3 \ , \\ \phi_2(\sigma_j) &= t_j[(\frac{\sigma_j}{t_j}) - 2(\frac{\sigma_j}{t_j})^2 + (\frac{\sigma_j}{t_j})^3], \\ \phi_3(\sigma_j) &= 3(\frac{\sigma_j}{t_j})^2 - 2(\frac{\sigma_j}{t_j})^3, \\ \phi_4(\sigma_j) &= t_j[-(\frac{\sigma_j}{t_j})^2 + (\frac{\sigma_j}{t_j})^3]. \end{aligned} \tag{17}$$

Substitution of the assumed solution into the equation of motion (13) leads to a non-zero error. The error for the assumed solution is "weighted" by multiplying by a set of test functions and setting the integral of the weighted error to zero to obtain two equations per element. The test functions are chosen to be the simplest possible, i.e. $\psi_1(\sigma_j) = 1$ (constant) and $\psi_2(\sigma_j) = \frac{\sigma_j}{t_j} - \frac{1}{2}$ (linear). The integral is taken over the time for each element, $t_j = t_c / E$, thereby dividing the time in-cut, t_c, into E elements. The resulting equations are [17]:

$$\begin{aligned} &\int_0^{t_j} \{M\left(\sum_{i=1}^{4} \mathbf{a}_{ji}^{n}\, \ddot{\phi}_i(\sigma_j)\right) + \mathbf{C}\left(\sum_{i=1}^{4} \mathbf{a}_{ji}^{n}\, \dot{\phi}_i(\sigma_j)\psi_p(\sigma_j)\right) + \\ &(\mathbf{K} - b\mathbf{K}_c(\sigma_j))\left(\sum_{i=1}^{4} \mathbf{a}_{ji}^{n}\, \phi_i(\sigma_j)\psi_p(\sigma_j)\right) \\ &+ b\,K_c(\sigma_j)\left(\sum_{i=1}^{4} \mathbf{a}_{ji}^{n-1}\, \phi_i(\sigma_j)\psi_p(\sigma_j)\right) - \\ &b\mathbf{f}_0(\sigma_j)\psi_p(\sigma_j)\}\, d\sigma_j = 0 \\ &p = 1,2 \end{aligned} \tag{18}$$

The displacement and velocity at the end of one element are set equal to the displacement and velocity at the beginning of the next. It is necessary to mention that in TFEA method with increasing the immersion (radial depth of cut), the cutting time increases and in order to converge a solution, the number of elements should be increased [24].

8. Prediction of Stability Lobes

The frequency domain method and TFEA are implemented using MATLAB software in order to obtain SLD. Parameters used for the simulations are given in table **3**.

Table (3): Cutting conditions and modal parameters.

Tool diameter	D=8mm
Number of tooth	N=2
Feed per tooth	F_t=0.1 mm
Cutting Coefficient	$K_t = 2\times10^8 N/m^2$ $K_n = 6\times10^8 N/m^2$
Modal Parameters	f_x , $f_y = 922\,Hz$ k_x , $k_y = 1.34\times10^6 N/m$ ξ_x , $\xi_y = 0.011$

The results of simulation for up-milling with 10%, 25% and 50% immersions are presented in figures **11-13**, respectively. The variation of spindle speed is chosen between 5000 rpm to 25000 rpm. The number of elements in TFEA method for the immersion above is set to 10, 20 and 30. For WOC=0.5D (50% radial immersion), both methods yield similar results. As radial depth of cut decreases, the discrepancy between the frequency domain method and TFEA in predicting stability boundaries grows considerably. The most prominent difference is the added set of lobes located at the odd integer fractions of twice the dominant eigen frequency, ($2f_t/(2k+1)$). These lobes are predicted only by the TFEA method and correspond to the period doubling (flip) bifurcation which causes periodic chatter [27].

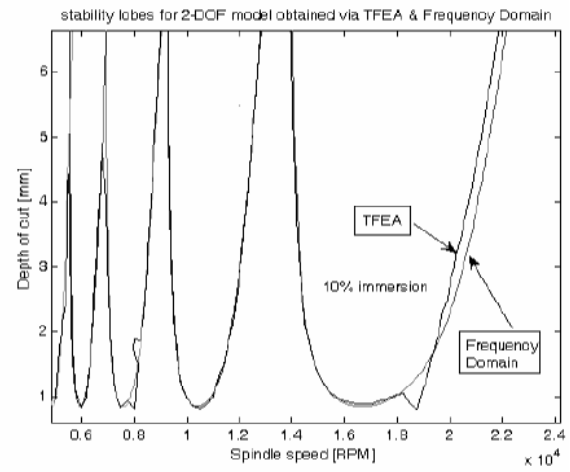

Fig. (11): stability lobes chart with two methods in 10% immersion.

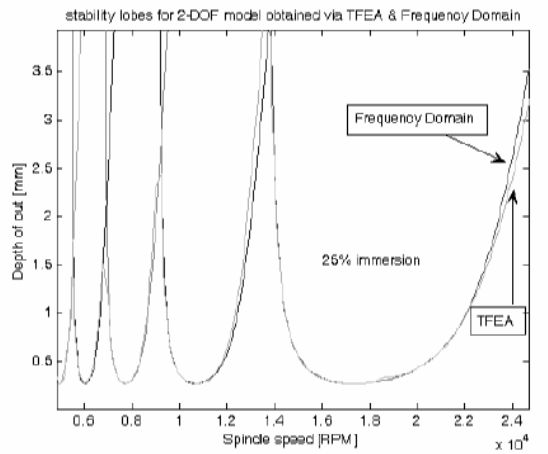

Fig. (12): stability lobes chart with two methods in 25% immersion.

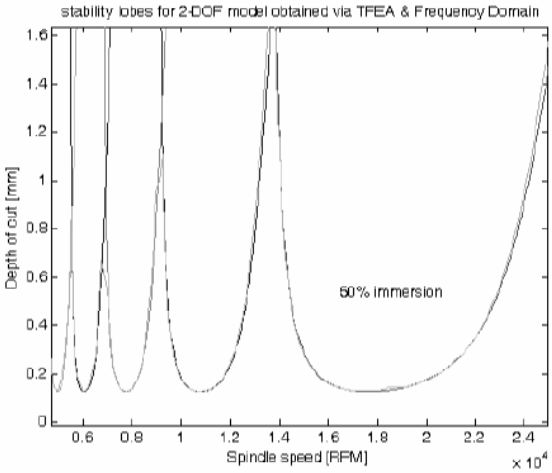

Fig. (13): stability lobes chart with two methods in 50% immersion.

9. Verification of Stability Lobes

In order to verify TFEA and frequency domain simulations, the Euler time domain simulations are used. That is a simple approach and also is has been a proven method for simulating the behavior of milling process [30-31].

The time domain simulations are performed for 5000, 5100, 5150 and 5200 rpm for different axial depths of cut. Fig. **14** compares the results obtained by the time domain simulation with the frequency domain method and TFEA. In the figure stable and unstable cutting conditions are identified by (O) and (*), respectively.

The stable and unstable cutting conditions are differentiated using FFT of the resultant force. F_x, F_y, x and y which obtained by simulation are also depicted. Fig. **15** depicts time histories and FFT of stable cutting conditions while Fig. **16** represents time histories and FFT of unstable cutting conditions.

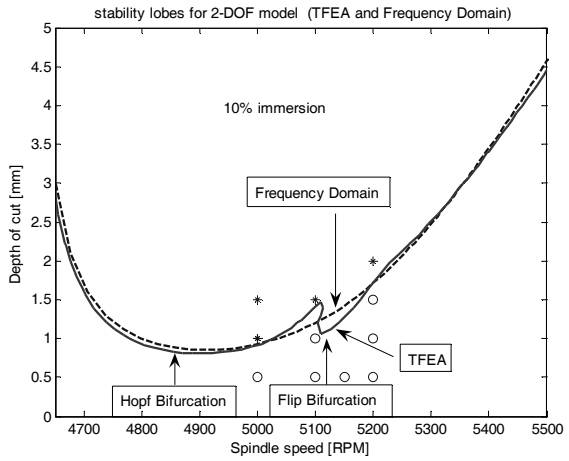

Fig. (14): stability lobes chart in 10% immersion for spindle speed between 4650rpm and 5500rpm.

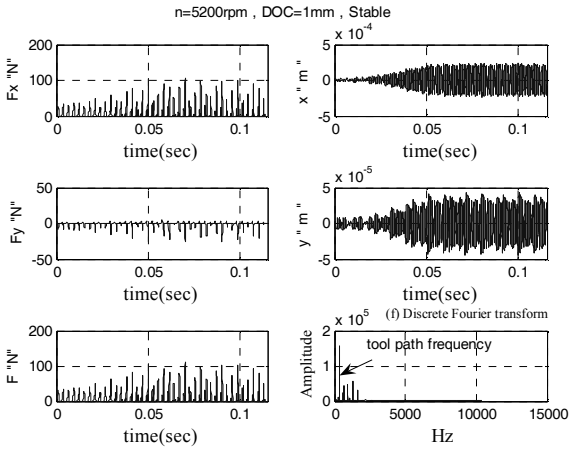

Fig. (15): up-milling, DOC =1 mm, n=5200rpm (stable cutting condition).

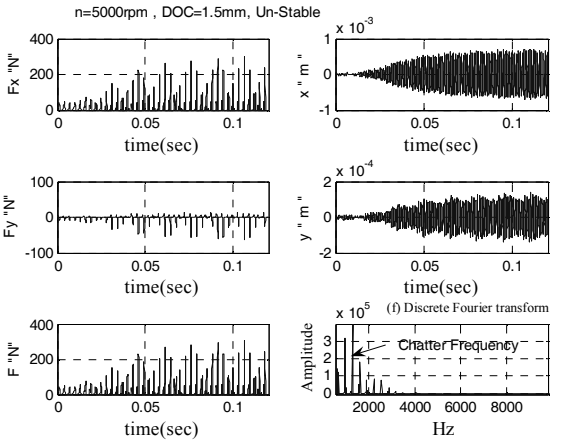

Fig. (16): up-milling, DOC =1.5 mm, n=5000rpm (unstable cutting condition).

10. Conclusions

In this research, milling cutting forces are evaluated, using analytical chip load algorithm and chip load calculated by ACIS. The predicted cutting forces are in a good accordance using both methods.

The effects of radial depth of cut and the axial one in cutting forces were studied and evaluated, It was illustrated that role of the radial depth in increasing the cutting forces is more pronounced than the axial depth of cut. Stability lobes for the up-milling case for various immersions are obtained using frequency domain and TFEA methods.

It is clarified that for large immersion (25% and 50% immersion), the stability lobe diagrams resulted from two methods of frequency domain and TFEA, are more or less identical, but with decreasing the immersion (10% immersion), the difference between the diagrams of the two methods is noticeable. Consequently, in low immersion milling, the TFEA method illustrates the Flip-Lobes, while this phenomenon is not observed in frequency domain method.

11. References

1. Caulfield, F.L. "Electromechanical Actuator Development for Integrated Chatter Prediction on High Speed Machining Centers", M.Sc. Thesis Mech. Eng. Dep't., North Caroling State Univ., 2002.
2. Modern Machine Shop 8/99 Online Supplement: www.mmsonline.com/articles/089903.html.
3. Smith, S. and Tlusty, J., "An Overview of Modeling and Simulation of the Milling Process", ASME J. Eng. for Industry, Vol. 113, No. 2, pp. 169-175, 1991.
4. Ehmann, K.F., Kapoor, S.G, DeVor, R.E., and Lazoglu, I., "Machining Process Modeling, A Review", ASME J. Manufacturing Science and Eng., Vol. 119, No. 1, pp. 655-663, 1997.
5. Corney, J. "3-D Modeling with ACIS Kernel and Toolkit", Heriot-watt Univ., 1997.
6. Tlusty, J. and Polacek, M., "The Stability of Machine-Tool against Self Excited Vibration in Machining", The Int. Research Conf. in Production Eng., ASME, Pittsburg, Pennsylvania, USA, 1963.
7. Tlusty, J., Zaton, W., and Ismail, F., "Stability Lobes in Milling", CIRP Annals, Vol. 32, No. 1, p. 309, 1983.
8. Tlusty, J., "Basic Non-Linearity in Machining Chatter", CIRP Annals, Vol. 30, No. 1, p. 299, 1981.
9. Solis, E., Peres, C.R. , Jime'nez, J.E., Alique, J.R., and Monje, J.C., "A New Analytical-experimental Method for the Identification of Stability Lobes in High-Speed Milling", Int. J. Machine Tools and Manufacture, Vol. 44, No. 2, pp.1591-1597, 2004.
10. Mann, B.P., Insperger, T.S., Bayly, P.V., and Stepan, G., "Stability of Up-Milling and Down-

Milling, Part 2, Experimental Verification", Int. J. Machine Tools and Manufacture, Vol. 43, No. 2, pp. 35–40, 2003.
11. Halley, J.E., "Stability of Low Radial Immersion Milling", M.Sc. Thesis, St. Louis, Mo, Mech. Eng. Dep't., Washington Univ., 1999.
12. Gradisek, J., Kalveram, M., Insperger, T., Weinert, K., Ste'pan, G. and, Grabec I.E. "On Stability Prediction for Milling", 2005.
13. Imani B.M. and Elbestawi, M.A. Geometric Simulation of Ball-End Milling Operations", Transactions of the ASME, J. of Manufacturing Science and Eng., Vol. 123, No. 1, pp. 177-184, 2001.
14. Philip V.B, Tony L.S., Brian P.M., David, A. Peters, and Gabor S., Tamas Insperger, Effects of Radial Immersion and Cutting Direction on Chatter Instability in End Milling, ASME Int. Mech. Eng. Conf., 2002.
15. Hartung, F., Insperger, T., Ste´pa´n, G., and Turi, J. "Approximate Stability Charts for Milling Processes Using Semi-discretization", Applied Mathematics and Computation, Vol. 174, No. 4, pp. 51–73, 2006.
16. Davies, M.A. and Balachandran, B., Impact Dynamics in Milling of Thin-Walled Structures, Non-linear Dynamics Vol. 22, No. 1, pp. 375–392, 2000.
17. Armorego E.J.A.. and Deshpande, N.D., "Force Prediction Models and CAD=CAM Software for Helical Tooth milling Processes. III. End-milling and Slot Operations", Int. J. Product Research, Vol. 32, No. 7, pp.1715–38, 1994.
18. Budak, E. Altintas, Y. and Armorego, E.J.A, "Prediction of Milling Force Coefficients From Orthogonal Cutting Data", ASME J. Manufacturing Science and Eng., Vol. 118, No. 1, pp.216–224, 1996.
19. Yoon, M.C. and Kim. Y.G., "Cutting Dynamic Force Modelling of End Milling Operation", J. Material Processing Tech., Vol. 155-156, No. 4, pp. 1383-1389, 2004.
20. Li, H.Z., Zhang, W.B., and Li, X.P., "Modelling of Cutting Forces in Helical end Milling, Using a Predictive Machining Theory", Int. J. Mech. Sciences, Vol. 43, No. 2, pp.1711–1730, 2001.
21. Moetakef-Imani, B., "Model Based Die Cavity Machining Simulation Methodology", PhD Dissertation, Mech. Eng. Dep't., McMater Univ., Hamilton, Canada, 1998.
22. Altintas Y., Budak E., "Analytical Prediction of Stability Lobes in Milling, Annals of the CIRP, Vol. 44, No. 1, pp. 357–362, 1995.
23. Mann, B.P., Bayly, P.V., Davies, M.A., and Halley J.E. "Limit Cycles, Bifurcations, and Accuracy of the Milling Process", J. Sound and Vib., Vol. 277, No. 4, pp. 31-48, 2004.
24. Insperger, T., Mann, B.P., Stepan, G., and Bayly, P.V. "Stability of Up-milling and Down-milling, Part 1, Alternative Analytical Methods", Int. J. Machine Tools and Manufacture, Vol. 43, No. 4, pp. 25-34, 2003.
25. Solis, E., Peres, C.R. , Jime´nez, J.E., Alique, J.R., and Monje, J.C. "A New Analytical–Experimental Method for the Identification of Stability Lobes in High-speed Milling", Int. J. Machine Tools and Manufacture, Vol. 44, No. 1, pp. 1591–1597, 2004.
26. Davies, M.A., Pratt, J.R., Dutterer, B., and Burns, T.J., "Stability Prediction for Low Radial Immersion Milling", J. Manufacturing Science and Eng., Vol. 124, No. 2, pp. 217–225, 2002.
27. Bayly, P.V., Halley, J.E., Davies, M.A., and Pratt, J.R., "Stability Analysis of Interrupted Cutting with Finite Time in the Cut", ASME, Manufacturing Eng. Division, Vol. 11, No. 1, pp. 989–996, 2000.
28. Bayly, P.V., Mann, B.P., Schmitz, T.L., Peters, D.A., Stepan, G., and Insperger, T., "Effects of Radial Immersion and Cutting Direction on Chatter Instability in End Milling", ASME Int. Mech. Eng. Conf. Exposition, No. IMECE-34116, New Orleans, LA, 2002.
29. Insperger, T. and Stépán, G., "Stability of High Speed Milling", AMD, Vol. 241, No. 3, pp. 119-123, 2000.
30. Schmitz T.L., "Recognition by a Statistical Evaluation of the Synchronously Sampled Audio Signal", The 2001 India–USA Symposium on Emerging Trends in Vibration and Noise Eng., Columbus, OH, 2001.
31. Schmitz, T.L.M. and Dutterer B.K. Exploring Once-per-revolution Audio Signal Variance as a Chatter Indicator", Machining Science and Tech., Vol. 6, No. 2, pp. 215–233, 2002.